PERGAMON

Planetary and Space Science 49 (2001) 327–336

Planetary and Space Science

www.elsevier.nl/locate/planspasci

The ionosphere of Ganymede

Aharon Eviatar[a], Vytenis M. Vasyliūnas[b,*], Donald A. Gurnett[c]

[a] *Department of Geophysics and Planetary Sciences, The Raymond and Beverly Sackler Faculty of Exact Sciences, Tel Aviv University, Ramat Aviv, Israel*

[b] *Max-Planck-Institut für Aeronomie, Max-Planck-Strasse 2, 37191 Katlenburg-Lindau, Germany*

[c] *Department of Physics and Astronomy, The University of Iowa, Iowa City, IA 52242, USA*

Received 16 December 1999; received in revised form 17 May 2000; accepted 12 July 2000

Abstract

We consider the distribution of plasma density in the atmosphere of Ganymede and present electron density profiles inferred from data of the Plasma Wave instrument of *Galileo*. To study the question of ionospheric plasma, we present a zero-dimensional local rate equation model of the source and loss functions and the atomic and molecular processes we assume to be taking place. We conclude from the model that Ganymede has a bound ionosphere composed mainly of molecular oxygen ions in the polar regions and of atomic oxygen ions at low latitudes and that protons are absent everywhere. This implies that the plasma observed to be flowing out along the open flux tubes connected to the polar cap is composed of ions of atomic oxygen. We predict that Ganymede is surrounded by a corona of hot oxygen atoms. The model neutral atmosphere has a composition similar to that of the ionosphere and is exospheric everywhere. Our calculated neutral column density is consistent with values of Ganymede ultraviolet auroral brightness observed by means of the Hubble Space Telescope.

1. Introduction

The icy Galilean satellites of Jupiter have atmospheres. The atmosphere of Europa has been modeled numerically in detail in 3-D by Saur et al. (1998) and their results are consistent with observation. Ganymede is significantly larger than the other satellites and, more importantly, has an intrinsic magnetic field as discovered by the *Galileo* spacecraft (Kivelson et al., 1996; Gurnett et al., 1996).

The earliest indication of a possible atmosphere at Ganymede was a stellar occultation observation by Carlson et al. (1973), who found an atmospheric pressure of the order of a microbar. Observations by the UVS (Ultraviolet Science) telescope of *Voyager 1* placed an upper limit on the pressure about five orders of magnitude lower (Broadfoot et al., 1981). Hubble space telescope (HST) observations by Hall et al. (1998) are consistent with the lower density, which is in contradiction to the early ionosphere/atmosphere model of Yung and McElroy (1977). Kumar and Hunten (1982) showed that the atmosphere can have two possible states that differ in pressure by a factor of 10^5. The uncertainties in the H_2O vapor pressure extrapolations are, according to Kumar and Hunten (1982), sufficient to leave indeterminate the differentiation between the high and low density states of the system. The latter is a regime in which the generation rate of the constituents of the atmosphere is easily accommodated by thermal escape. As we shall see below, the HST observations fit the low-density state model of Kumar and Hunten (1982).

In this paper, we shall attempt to evaluate the distribution of plasma density in the exospheric ionosphere in both the polar cap and the equatorial regions of Ganymede. We also present new *Galileo* plasma wave science (PWS) measurements that have implications for the nature of the ionosphere. A simple steady-state analytic model is developed for Ganymede, which is consistent with the findings of PWS and HST but raises severe questions with respect to published interpretations of Plasma Science (PLS) data. We find the latter to be inconsistent with the physical processes that must be taking place at and near the surface of Ganymede.

2. The observations

In this section, we shall first present the PWS data obtained during the Ganymede 1 and Ganymede 2 (hereafter G1 and G2, respectively) encounters and then

* Corresponding author. Tel.: +49-5556-979-435; fax: +49-5556-979-169.

E-mail address: vasyliunas@linmpi.mpg.de (V.M. Vasyliūnas).

0032-0633/01/$ - see front matter
PII: S0032-0633(00)00154-9

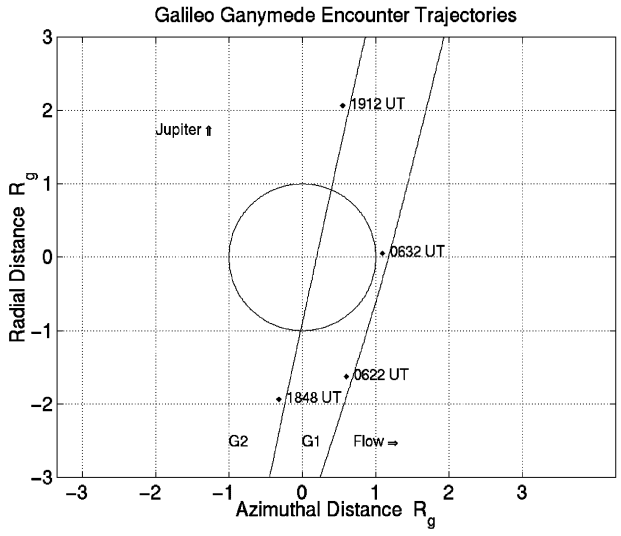

Fig. 1. Horizontal projection of the G1 and G2 encounters of *Galileo* with Ganymede.

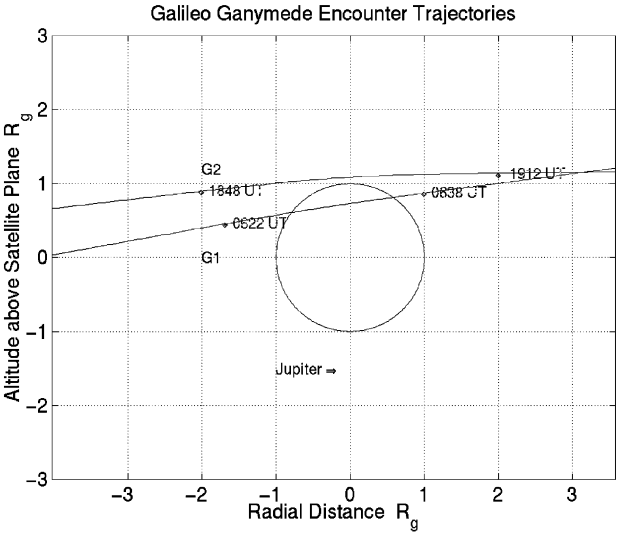

Fig. 2. Vertical projection of the G1 and G2 encounters of *Galileo* with Ganymede.

discuss the published *Galileo* Ultraviolet Science (UVS) and PLS data.

We also quote data and inferences from the energetic particle detector (EPD), radio occultation studies, ground based observations and HST findings. The implications of the combined data sets will be shown to be consistent with our model. The horizontal and vertical projections of the encounter trajectories are shown in Figs. 1 and 2.

2.1. PWS data

Fig. 3 shows the electron density obtained from PWS measurements of the upper hybrid resonance frequency during the G1 and G2 flybys. For a discussion of the technique

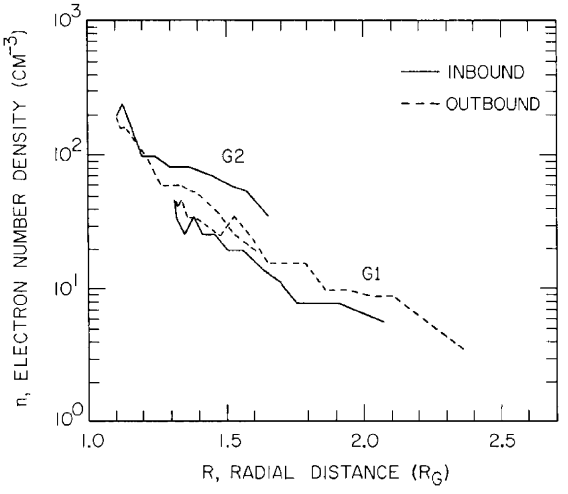

Fig. 3. Electron density profiles on Ganymede 2 obtained by means of the PWS instrument on *Galileo*.

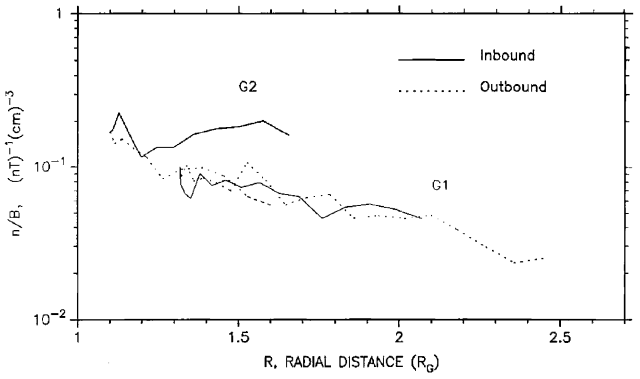

Fig. 4. The ratio of density to magnetic field magnitude as measured by the MAG and PWS instruments on *Galileo*.

involved, see Gurnett et al. (1996). The densities are derived from the density-dependent upper hybrid resonance and are accurate to the level of the channel separation, i.e. about 6%. The G1 inbound and outbound curves and the G2 outbound share a more or less common slope over most of the range and the steepening of the slope shown by G2 inbound is based on too little data to be considered real. The common slope of the first mentioned triad corresponds to a scale height of 600 km and a surface density of about 400 cm^{-3}. We shall conclude below that very near the surface, the scale height may be expected to be considerably smaller, and the surface density correspondingly greater, but nonetheless, our predicted density will be well below the upper limit of 4×10^3 cm^{-3} obtained by Kliore (1998) in the radio occultation observation. This density should be approximately equal to the density of O_2^+, since atomic oxygen is a minor constituent of the bound ionosphere, as we show in Section 4.2.

In Fig. 4, we plot the ratio of density n to magnetic field magnitude B as measured by the magnetometer and PWS instruments on *Galileo* as a function of radial distance along

a field line. For the case of plasma flowing outwards along magnetic field lines at a constant speed, it follows from the continuity and magnetic field divergence equations:

$$\nabla \cdot (n\mathbf{U}) = 0,$$
$$\nabla \cdot \mathbf{B} = 0 \quad (1)$$

that the ratio n/B is constant along a field line. We may note with the exception of the anomalous G2 inbound curve, that, although the ratio is not constant but decreases with increasing radial distance, its variation is much smaller (about a factor of 10 over the range of observations) than the variation of n itself (about a factor of 70). The implications of this phenomenon for the outflow from the polar cap will be discussed below in Section 4.2.

2.2. Other Galileo observations

The *Galileo* ultraviolet instrument observed, during the G2 encounter, a cloud of neutral atomic hydrogen in Ly $-\alpha$ emission with a modeled density of about 10^4 cm^{-3} at the surface, an inverse square radial dependence or a scale length of about a Ganymede radius (2634 km) (Barth et al., 1997). This is consistent with a source-free, spherically symmetric, constant velocity outflow, i.e. the continuity equation for this case is

$$\frac{\partial}{\partial r}\left(r^2 u_r n(r)\right) = 0 \quad (2)$$

which implies the r^{-2} fall off.

At the G2 encounter, Frank et al. (1997) reported an outflow of ions which they assume to be protons with a density of about 100 cm^{-3}, a bulk velocity component of about 70 km/s and a temperature of the order of 1–3 eV. These densities were consistent with the G1 density measurements reported by Gurnett et al. (1996). On the other hand, Barth et al. (1997) point out the difficulties in supplying the protons mentioned by Frank et al. (1997). An alternative hypothesis, that protons are sputtered directly from the surface, fails because the rate of such sputtering is at least 3–4 orders of magnitude smaller than the neutral sputtering rate (Johnson, 1990). As we shall demonstrate below, there are no protons in the ionosphere of Ganymede (nor would we expect to find them at Europa). An alternative interpretation to the results reported by Frank et al. (1997) is presented in detail in a separate paper (Vasyliūnas and Eviatar, 2000).

The polar caps of Ganymede are heavily sputtered, as indicated by the surface characteristics (Johnson, 1997; Pappalardo et al., 1997) and the *Galileo* heavy energetic ion observations (Paranicas et al., 1999). The change in color of the terrain and the boundary of closed field lines, as inferred from the EPD and magnetometer measurements (Williams et al., 1997; Kivelson et al., 1998) appear to coincide quite well. Paranicas et al. (1999) estimate a polar cap source strength of 2.6×10^{26} s^{-1}. The lower latitude regions show molecular oxygen and ozone in the form of liquids (Calvin et al., 1996; Hendrix et al., 1999; Johnson and Jesser, 1997) although there are indications of ion radiation effects there as well (Hendrix et al., 1999).

Hall et al. (1998) report the detection by means of HST of ultraviolet airglow in the polar regions of Ganymede in the atomic oxygen lines at 130.4 and 135.6 nm with an intensity of 300 R (1 Rayleigh $= 10^6$ photons cm^{-2} s^{-1}) in the northern hemisphere and 100 R in the south polar cap region. They interpreted this in the light of the G1 PWS data, taken at a greater distance from the surface of Ganymede (Gurnett et al., 1996), that showed $n_e \approx 100$ cm^{-3}, to be consistent with a surface column density in the range 10^{14}–10^{15} cm^{-2}. At the G2 encounter, as shown in Section 2.1, a higher electron density was found. The surface plasma density is not as well constrained and an upper limit of 4×10^3 cm^{-3} has been estimated by means of radio occultation measurements (Kliore, 1998). Later observations by Feldman et al. (2000) detected a high degree of inhomogeniety in the emitted brightness which leads to the conclusion that the radiation is auroral in nature.

3. Composition and sources

The existence of an indigenous atmosphere entails the presence of an ionosphere as well. Sputtering, even in the absence of major sublimation, can deliver molecules to the space above the surface and, if conditions are favorable, support a significant atmosphere. As mentioned above, the existence of a molecular oxygen atmosphere on both Europa and Ganymede has been established (Hall et al., 1995, 1998). In this section, we explore the sources and the physical mechanisms that lead to the composition of the ionosphere of the Ganymede.

3.1. Physical processes

In the sputtered region the products of the interaction will depend on the energy of the incident ions. The polar cap temperatures, which are too low to support effective sublimation, will also cause any sputtered water vapor and hydroxyl to recondense before it can dissociate. Molecular oxygen, on the other hand, can maintain a vapor pressure even at polar cap and nightside temperatures, with the result that there is gaseous O_2 available for interaction with plasma and energetic particles (Johnson, 1996).

In the tropical and equatorial region, the situation is quite different. Water vapor and hydroxyl can survive in the atmosphere and on photodissociation, the hydrogen escapes forthwith, while the oxygen atom comes off with a very low velocity (Budzien et al., 1994) and thus does not escape as in the polar cap region. Energetic electrons in the range in which the fluxes are significant do not have access to this closed field line region (Eviatar et al., 2000) and the atomic oxygen should mainly be a product of photodissociation. The vast majority of the atomic oxygen photodissociation

of O_2 is in the ^1D state and 14% of that made by H_2O photodissociation is in that state as well (Huebner et al., 1992).

Low-energy sputtering experiments (0.5–6 keV) by Bar-Nun et al. (1985) indicate that O_2 and H_2 are produced in the body of the ice, whereas water vapor and H are produced near the surface. Bar-Nun et al. (1985) find that the sputtering of water vapor and of atomic hydrogen are temperature independent and of comparable magnitude, which they interpret to imply that H is created by the breaking of water molecule bonds at the surface at a rate comparable with the sputtering of water. The emitted hydrogen, molecular and atomic, will escape rapidly, since the energy required to escape from the surface of Ganymede is $E_L = 0.039$ eV/amu, which is readily available to sputtered low-mass products. Energy in excess of E_L is also available to the low-mass dissociation products of water vapor (Budzien et al., 1994) and hydroxyl (van Dishoeck and Dalgarno, 1984) as may be noted in Table 1, and to oxygen atoms from dissociation of O_2 in low states of excitation. As mentioned above, the molecular oxygen will survive both recondensation ($T \geqslant 80$ K) and escape loss. Water vapor and the hydroxyl remaining behind from the dissociation in the ice surface will recondense under the low-temperature conditions of the polar cap environment. The yield of O_2, created by oxygen recombination reactions in the ice (Bar-Nun et al., 1985), is comparable to the water yield and the molecular oxygen from this source, which lacks the energy needed to escape from Ganymede in significant amounts (Sieveka and Johnson, 1982), will survive in gaseous form in the atmosphere. At higher incident ion energies (up to a few MeV), H_2O, O_2 and H_2 are produced (Johnson, 1990; Johnson and Quickenden, 1997) and will be subject to the same loss processes.

The time to escape to the distance of the magnetopause ($2R_g$)

$$t = \int_{R_g}^{2R_g} \frac{dr}{\sqrt{v_0^2 - v_\infty^2 + 2GM/r}}, \leqslant 1000 \text{ s}.$$

(v_0 and v_∞ are the surface and escape speeds respectively, G is the gravitational constant and M is the mass of Ganymede) is two or three orders of magnitude shorter than either the photoionization or electron impact ionization time of atomic hydrogen, as may be noted by glancing at Table 1.

The electron impact ionization rates given in Table 1 are for 50 eV electrons. Laboratory work (Shulman et al., 1985) indicates that the rates of the dissociation and excitation processes that give rise to these emissions peak between 50 and 100 eV. There are no published electron spectra from Galileo below 800 eV, but Voyager results indicate a bimodal distribution with a core at about 20 eV and a hot component of about 1/10 the density at 2 keV (Scudder et al., 1981). The value of 50 eV is taken for illustrative purposes and the conclusions would be no different for 100 eV. Even if the suprathermal electron density were as high as 100 cm^{-3}, huge compared to observed plasma sheet densities, it is clear that no significant ionization of the hydrogen population can take place in the time available. *We infer from this that protons are not present in the ionosphere of Ganymede.* The implications of this conclusion are discussed below in Section 4.2.

Although the allotropes of hydrogen escape readily and O_2 remains, it should not be inferred that huge amounts of oxygen will accumulate on the surface, as has been suggested by Frank et al. (1997). The molecular oxygen is subject to ionization and dissociative excitation by the Jovian plasma sheet electrons and to loss by means of the kinetic energy made available to the dissociation products by dissociative recombination:

$$\begin{aligned} &O_2 + e \rightarrow O + O + e, \\ &O_2 + e \rightarrow O_2^+ + e + e, \\ &O_2^+ + e \rightarrow O + O. \end{aligned} \quad (3)$$

The dissociation reactions are both exothermic, and the excess energy can be delivered to the atomic oxygen as kinetic translational energy, i.e., the atomic oxygen escapes, or as excitation energy of the electrons in the product atom, in which case a UV photon is emitted and the atoms remains bound and available for ionization. The dissociative ionization process, which produces an ionosphere ion–electron pair directly is possible, but is much slower (Schmidt et al., 1988) and will therefore be ignored. The parameters relevant to these reactions and the associated rate equations are given in Table 1. We shall see below how these processes combine to create the observed configuration.

Nagy et al. (1998) predict that Europa has a corona of hot oxygen, with the energy for the escaping atoms provided by the dissociative recombination of O_2^+. It is quite reasonable, in light of the above to expect such a cloud to envelope Ganymede as well. Hall et al. (1998) show, on the basis of emission line ratios, that the UV emission from atomic oxygen observed by means of HST is produced by electron impact dissociation of molecular oxygen, i.e. of the first of the reactions (3). It has been found, however (Shulman et al., 1985) that for incident electron energy greater than about 50 eV, the main channel of this reaction involves an initial ionization followed by immediate dissociative recombination. We thus may use the energy level branching ratios of Kella et al. (1997) cited by Nagy et al. (1998) for the atmosphere of Europa to infer a similar result for Ganymede. A search for the radiative signature of such an oxygen corona would be a worthy effort.

3.2. Model equations

In the following model, we shall assume that all electron ionization and subsequent dissociative recombination of molecules lead to escape. For the case of electron impact dissociation of O_2, the fraction excited to sufficiently high energy will emit the UV lines and the remainder will escape,

Table 1
Parameters for molecular and atomic processes

Process	ΔE^a (eV)	Rate coefficient	References
H_2O photodissociation	5	3.7×10^{-7} s^{-1}	Budzien et al. (1994)
O_2 photodissociation	1.3	4.0×10^{-6} s^{-1}	Schmidt et al. (1988)
OH photodissociation	3.0	1.5×10^{-7} s^{-1}	van Dishoeck and Dalgarno (1984)
O_2 electron dissociation	5.12	1.3×10^{-8} cm^3 s^{-1}	Cosby (1993)
O_2 electron ionization	12.1	3.2×10^{-10} cm^3 s^{-1}	Schmidt et al. (1988)
O_2^+ dissociative recombination	5	5.0×10^{-7} cm^3 s^{-1}	Walls and Dunn (1974)
H electron impact ionization	—	2.54×10^{-8} cm^3 s^{-1}	Lotz (1967)
O electron impact ionization	—	4.24×10^{-8} cm^3 s^{-1}	Lotz (1967)

[a]Dissociation energy.

including the large fraction excited to the ^{1}D level. We are aware of the limitations of this assumption, which ignores cascade decay to the ^{1}D level from the 115.2 nm level.

In light of the above, we may set up a simple, illustrative zero-dimensional model (Richardson et al., 1998) for the density and composition of the ionosphere. Since hydrogen, both molecular and atomic, escapes, the relevant species are H_2O, O_2, OH, O and O^+ at low latitudes and O_2 and O and their ions in the polar cap region. For a neutral atmosphere in equilibrium with a surface at a temperature of about 120 K in the region poleward of 45° (Orton et al., 1996), the scale height of O_2, is $H_{O_2} = 21.5$ km. The usually invoked doubling of the scale height for a singly ionized particle by the ambipolar field is based on the assumption of no net outflow, which does not apply in this situation. In our model, we use H_{O_2} to define the volume in which the sputtering takes place and the effective electron scale height, $H_e = 600$ km, is estimated from Fig. 3 as a measure of the depletion length over which the UV radiation is excited by electron impact dissociation (Hall et al., 1998).

The resulting rate equations are, in generic form

$$\frac{dn_j^{(m,n)}}{dt} = f_j^{(m,n)} - \left[(\alpha_j + \beta_j)n_e + \eta_j^{(i)} + \eta_j^{(d)} + v_j \sum_k \sigma_{jk} n_k^{(a+m,i)} + \delta_j^{(m,n)}\right] n_j^{(m,n)},$$

$$\frac{dn_j^{(m,i)}}{dt} = \left[\alpha_j n_e + \eta_j^{(i)} + v_j \sum_{j\neq k} \sigma_{jk} n_k^{(a+m,i)}\right] n_j^{(m,n)} - \left[v_j \sum_{k\neq j} \sigma_{kj} n_k^{(a+m,n)} + \gamma_j^{(d)} n_e + \delta_j^{(m,i)}\right] n_j^{(m,i)},$$

$$\frac{dn_j^{(a,n)}}{dt} = \sum_k (\beta_k n_e + \eta_k^{(d)}) n_k^{(m,n)} - \left[(\alpha_j + \beta_j)n_e + \eta_j^{(i)} + v_j \sum_k \sigma_{jk} n_k^{(a+m,i)} + \delta_j^{(a,n)}\right] n_j^{(a,n)},$$

$$\frac{dn_j^{(a,i)}}{dt} = \left[\alpha_j n_e + \eta_j^{(i)} + v_j \sum_{j\neq k} \sigma_{jk} n_k^{(a+m,i)}\right] n_j^{(a,n)} - \left[v_j \sum_{k\neq j} \sigma_{kj} n_k^{(a+m,n)} + \delta_j^{(a,i)}\right] n_j^{(a,i)}, \quad (4)$$

where the following notation has been used: The subscripts j and k denote individual species, the superscripts $(m,n), (m,i), (a,n)$, and (a,i) denote molecules, neutral and ionized and atoms, neutral and ionized, respectively. We designate charge exchange cross-sections as σ_{kj}, electron ionization rate coefficients by α_j, electron dissociation rate coefficients by β_j, photodissociation and photoionization rates by $\eta_j^{(i)}$ and $\eta_j^{(d)}$, respectively, and the dissociative recombination rate by $\gamma^{(d)_j}$. Dissociation of molecules by any process will engender various products, which may be atoms or molecules of lower order. To avoid confusion, the number of product atoms from a given dissociation process is considered to be included in the β and η terms and will be applied ad hoc for the species being deal with. The $\delta_j^{(p,q)}$ terms represent the escape rates of the specific species and are of the form: $\delta_k^{(p,q)} = v_k^{(p,q)}/H_k$.

The source strengths for the sputtered species $f_i^{(p,q)}$ are given for the polar cap by

$$f_i^{(p,q)} = \frac{F_i^{(p,q)}}{2\Sigma_1 H_i},$$

where Σ_1 is the combined area of the two polar caps $\lambda \geqslant 45°$ of Ganymede, 2.6×10^{17} cm^2 and in the tropics by the sublimation flux [Alexander et al., 1999]

$$j_w \approx 10^9 \text{ cm}^{-2} \text{ s}^{-1}.$$

We include charge exchange as a neutral loss mechanism since the newly created neutral has sufficient velocity to escape but it is not a source of ions since ion number is conserved in charge exchange reactions. The values of these various rate coefficients are given in Table 1. For the steady state in which all the time derivatives in Eqs. (4) vanish, the values of these rate coefficients do not matter except to show that they are large enough to preclude any contribution to the plasma density from the creation of protons. We also include no rate equations for hydrogen allotropes because

of the arguments given above. In the following sections, we proceed to apply this model to the objects under consideration. We calculate predicted neutral and ion densities and compare them with the PWS and HST observations.

4. Ion densities

We consider two separate regions on the surface of Ganymede, the polar cap region, for which the latitude $\lambda > 45^\circ$ and the lower latitude regions equatorward of this limit. Temperature maps published by Orton et al. (1996) show a range of temperatures from about 150 K in the subsolar equatorial zone to below 90 K near the poles and in the pre-dawn sector. For the low temperatures in the polar cap region, all sputtering products can be expected to recondense immediately with the exception of molecular oxygen which can survive as gas down to a temperature of 80 K (Johnson, 1996). In the lower latitude dayside regions, where temperatures are significantly higher and Ganymede has closed field lines, we expect the main contribution to the gaseous atmosphere at Ganymede to be from sublimation (Alexander et al., 1999). In this region water group molecules such as H_2O and OH will survive above the surface and will participate in the local atmospheric chemistry. As we shall see below, this difference will give rise to a difference in composition between the polar and equatorial ionospheres.

4.1. The polar caps

In the appendix, we derive expressions for the densities of the four components of the Ganymede polar ionosphere and atmosphere. For the values of the parameters given above, we find for the molecular neutrals and ions:

$$n_{O_2^+} = 2.2 \times 10^3 \text{ cm}^{-3},$$

$$n_{O_2} = 3.5 \times 10^6 \text{ cm}^{-3},$$

$$n_{O^+} = 3.3 \times 10^2 \text{ cm}^{-3},$$

$$n_O = 1.7 \times 10^6 \text{ cm}^{-3}, \quad (5)$$

which leads, with the scale height H_{O_2} to a molecular oxygen column density

$$N_{O_2} = 7.4 \times 10^{12} \text{ cm}^{-2}. \quad (6)$$

This is somewhat less than the column density estimated by Hall et al. (1998), who used a lower value for the electron density. We also find a higher atomic oxygen abundance than postulated in the analysis of Hall et al. (1998). The value estimated here is certainly consistent with the *Voyager* occultation constraint of an atmospheric density of less than 1.5×10^9 cm^{-3} (Broadfoot et al., 1981). The plasma density is considerably higher (by a factor of about 5) than that extrapolated above from the curve in Fig. 3, which casts some doubts, as expressed above in Section 2.1 on the validity of the extrapolation of the scale height observed a few hundred kilometers above the surface to the near-surface region. The PWS result and the total ion density (atomic oxygen ions comprise only about 15% of the plasma and can be regarded as a minor component) can be reconciled if we assume a mean scale height in the intervening layer of about 125 km. Further speculation is, in our opinion, fruitless in view of the vast uncertainties in both the atomic and environmental parameters. It certainly does not contradict the upper limit of Kliore (1998).

It is of interest to attempt to predict the auroral emission to be expected from the above model atmosphere. The expression that relates the product of the electron and molecular oxygen density to the observed UV emission:

$$4\pi I = \int_0^\infty c_2 n_e n_{O_2} \, ds = c_2 n_e n_{O_2} H_{O_2}. \quad (7)$$

In the notation of Hall et al. (1998),

$$c_2 = 1.1 \times 10^{-9} \text{ cm}^3 \text{ s}^{-1}$$

is the rate coefficient for excitative dissociation into the ^{5}S state. Use of the model results given in Eq. (5) leads to the brightness

$$4\pi I = 20R, \quad (8)$$

which is about an order of magnitude less than the brightness reported by Hall et al. (1998). More recent measurements with higher spatial resolution of Feldman et al. (2000) show a great degree of inhomogeniety in the longitudinal and latitudinal distribution of the auroral brightness with maxima in "hot spots" of about 300R in the vicinity of 45° and strong dropoffs with increasing latitude. The "mean" brightness in the Feldman et al. (2000) polar regions show upper limits of 50R in much of the region with values as large as 100–150R in the outer peripheries of the bright spots. Obviously a simple model such as ours that assumes polar cap uniformity cannot be expected to reproduce the details of the auroral structure and it is reasonable that our "mean" value be significantly lower than the maxima observed. Further analysis of the structure of the upper polar atmosphere and ionosphere and the spatial distribution of aurora will depend on finding the pitch angle and energy space distribution functions of the electrons responsible for the processes taking place.

4.2. The polar cap outflow

The polar wind is a known terrestrial phenomenon, the ambipolar outflow of thermal ions in the polar ionosphere, driven by the escape of the electrons. At the Earth, the light minor ion of hydrogen is driven to supersonic speed by the ambipolar field between the electrons and the atomic oxygen. As we have shown above, the situation in the polar cap region of Ganymede is somewhat different since there are no protons. On the other hand if the density of atomic

oxygen plasma is indeed small compared to that of O_2^+, it may well be that something analogous to a polar wind flow is taking place. Of course, *Galileo* is not moving along a stream line, in which case n/B would be conserved, but the approximate constancy of this ratio shown above in Fig. 4 is highly suggestive of such a polar wind like outflow.

In this region we have electrons bound by the ambipolar electric field to ions of mass 32, i.e. their effective mass would be 16 if the ambipolar approximation were to hold. The minority ion, O^+ would then experience an electric field that very nearly cancels its gravity. The motion of the particle along the field would than depend on residual pressure gradient effect. In the direction normal to the magnetic field, it will have whatever pickup velocity the attentuated corotation flow might give it. In contrast to protons at the Earth, whose mass in only 1/8 that of the majority heavy ion, the O^+ would not, in the ideal situation of pure ambipolar diffusion and equal ion and electron temperatures, experience any acceleration and the velocity along the field line would be totally unconstrained. A flow velocity of about 18 km/s has been inferred from published PLS observations by Vasyliūnas and Eviatar (2000). Motion perpendicular to the field line will be driven by the corotation electric field. Upper limits of the order of 25 km/s have been set from the EPD anisotropies by Williams et al. (1998) and the velocity will be much smaller if Ganymede has a high conductance (Eviatar et al., 2000).

In addition to the plasma outflow, neutral atomic oxygen created in the ground state or in low excited states will escape in a manner analgous to the escape of hydrogen discussed above. We predict that these escaping atoms will give rise to an oxygen corona around Ganymede analogous to the hydrogen corona observed there (Barth et al., 1997; Feldman et al., 2000) and predicted for Europa by Nagy et al. (1998). Atoms created in a high excited state, such as that which gives the observed oxygen ultraviolet airglow, have small translational energy and are gravitationally bound.

5. The closed field line region

During encounter G8, the spacecraft entered a region of closed field lines as indicated by the detection of trapped energetic electrons (Williams et al., 1997) and the magnetometer measurements by Kivelson et al. (1998). In this region, the energetic particle spectra change drastically (Eviatar et al., 2000). The magnetospheric thermal plasma density can be expected to be very low in this region, because of the inaccessibility of closed drift paths to injected Jovian particles (Eviatar et al., 2000; Volwerk et al., 1999) and the paucity of local plasma sources, as shown in the previous section.

In the low-latitude regions of Ganymede, the dayside temperature can be as high as 140–150 K (Orton et al., 1996) and a vapor pressure of water can be maintained above the ice. Alexander et al. (1999) have estimated the sublimation flux of water vapor to be as high as $j_w = 10^9$ cm^{-2} s^{-1}. For the equatorial belt between north and south latitudes of 45°, with area $\Sigma_2 = 6 \times 10^{17}$ cm^2 this can reach a dayside source strength of 6×10^{26} s^{-1}. Nonetheless, the arguments presented above against the existence of hydrogen in the Ganymede tropical atmosphere for times long enough to allow protons to be created still hold. Thus we have a system of equations similar to (4) with the addition of a rate equation for water vapor and, since the oxygen ions are constrained to move along the closed field lines, the replacement of the plasma sink term with a term of the form

$$\psi = \sigma_s v n_O,$$

where $\sigma_s = 5 \times 10^{-15}$ cm^{-2} (Book, 1977), representing collisional pitch angle diffusion of the oxygen ions into a loss cone in which they will collide with the surface of Ganymede.

In the appendix, we apply Eqs. (4) to this situation and obtain the set of Eqs. (A.3). We have left out equations for hydrogen, which has escaped, and for molecular oxygen and ozone, which do not exist in gaseous form in this region (Hendrix et al., 1999). We have kept charge exchange between neutral and ionized oxygen as a loss mechanism for neutrals, on the assumption that the former ion now released from the control of the magnetic field has sufficient energy (0.6 eV) to escape and have made allowance for the fact that H_2O^+ is lost via the combined reactions of ion–atom interchange and dissociative recombination of the product H_3O^+

$$H_2O + H_2O^+ \rightarrow H_3O^+ + OH,$$

$$H_3O^+ + e \rightarrow H_2 + OH. \quad (9)$$

The hydrogen escapes and the hydroxyl remains to undergo photodissociation and thus contribute more bound oxygen atoms. Because of the efficiency of dissociative recombination of all the molecular ions and the effectiveness of photodissociation of neutral molecules, the dominant ion in this part of the ionosphere is O^+ and charge neutrality implies

$$n_e \approx n_{O^+}.$$

Application of the assumptions that:

- Photolysis and photoionization dominate all atomic and molecular processes.
- The dominant channel for photodissociation of water vapor is

$$H_2O + \hbar\omega \rightarrow H + OH.$$

- The cross-sections for pitch angle scattering and charge exchange are approximately equal (value given in text) and the typical ion speed is about 1 km/s

and use of the Eqs. (A.3), leads, as shown in the Appendix, to the values

$$n_{O^+} = \frac{\eta_O^i}{\psi_s} = 3.7 \times 10^3 \text{ cm}^{-3},$$

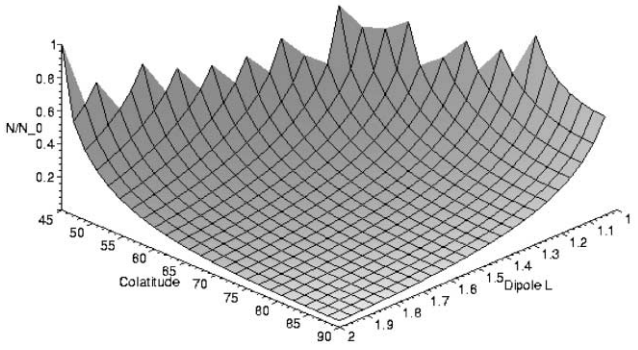

Fig. 5. Normalized plasma density in the closed field line region.

$$n_O = \frac{J_{H_2O}}{\eta_O^i/\psi_s H_{H_2O}(\sigma_{O+O} v + \psi_s)} = 5.6 \times 10^7 \text{ cm}^{-3}, \quad (10)$$

which for a neutral oxygen scale height of 54 km leads to a column density

$$N_O = 3 \times 10^{14} \text{ cm}^{-2},$$

significantly larger than the O_2 column density predicted by our model for the polar cap region, but still nearly exospheric. The main source of atomic oxygen in this model is photolysis of water and hydroxyl, a process that populates the ^1D level heavily. The observation of 630 and 636.3 nm emission reported by Brown and Boucher (1999) may be construed to provide support for our conclusions.

It is of interest to calculate the variation of the ion density along a closed field line. This has been done for a nonrotating Earth (which corresponds to Ganymede with appropriate scaling) by Eviatar et al. (1964). Their expression, which includes the effect of gravity and the magnetic mirror force for an ion exosphere can be written, in the following form, normalized to the surface density on a given L shell:

$$\frac{n(r,L)}{n(1,L)} = \left(1 - \left(1 - \frac{B}{B_0}\right)^{1/2} \exp\left[-\frac{\beta B(1 - R_g/r)}{(B_0 - B)}\right]\right) \times \exp\left[-\frac{\beta B(1 - R_g/r)}{(B_0 - B)}\right], \quad (11)$$

where β is the Jeans escape parameter (the ratio between the escape and thermal energies for the species in question), B is the magnitude of the dipole field and B_0 is surface field. We plot this expression Fig. 5 as a function of bothy colatitude and L, in order to display the full dimensionality of the variation. The relative density in the closed field line region drops off very rapidly from its surface value, which lends support to the conclusion of Volwerk et al. (1999), inferred from both drift trajectories and field line resonances, that the plasma density in this region must be very low.

6. Conclusions

We have presented observations of the radial profile of the electron density in the near-Ganymede polar cap region from the G1 and G2 flybys. The n/B ratio computed from these profiles is indicative of a polar cap outflow. We have developed a simple rate equation model that predicts an ionosphere on Ganymede comprised of oxygen ions, with molecular oxygen dominant in the polar region and atomic oxygen in the equatorial zone. The predicted neutral composition in both regions is similar. Our model results are consistent, within the uncertainties of the ambient parameters, in particular the unknown electron temperature, with the UV auroral observations made by HST (Hall et al., 1998; Feldman et al., 2000). We have shown that the conditions holding over the entire surface of Ganymede are inconsistent with the existence of protons, reported by Frank et al. (1997), whose observation of an outflow of charged particles from the polar cap region during the G2 flyby must, therefore, be reinterpreted as an outflow of atomic oxygen ions at a much lower flow speed. (see Vasyliūnas and Eviatar (2000) for a detailed discussion). We also predict that Ganymede should be enveloped in a corona of atomic oxygen escaping from the polar cap and suggest that a spectroscopic search for it would be a worthy effort.

We analyze the configuration in the region of closed field lines traversed by *Galileo* during G8 and apply a Earth-derived model of Eviatar et al. (1964) to map the exospheric density along the field lines. We find that the density should drop off quite rapidly which lends support to the prediction by Volwerk et al. (1999) that the ion density should be very low.

Acknowledgements

We gratefully acknowledge helpful discussions with W.S. Kurth, M.A. McGrath, R.E. Johnson, P.D. Feldman, D.F. Strobel, L.J. Paxton and M.E. Brown. We are grateful to M.G. Kivelson for her gracious permission to use the magnetometer data upon which Fig. 4 is based. The work at Tel Aviv University and at the Max-Planck-Institut für Aeronomie was sponsored in part by the German–Israel Foundation for Basic Research (GIF) under grant I-562-242.07/97. The research at the University of Iowa was supported by NASA through JPL contract 958779. The final revision of this paper was carried out while A. Eviatar was a visitor at the Hubble Space Telescope Science Institute in Baltimore MD, USA. Their hospitality is gratefully acknowledged.

Appendix A. Specific density equations

A.1. The polar regions

For the polar regions, we can formulate the appropriate rate equations from (4) for O_2, O_2^+, O and O^+. We thus

obtain in terms of the generic Equations (4):

$$
\begin{aligned}
&(\alpha_{O_2}+\beta_{O_2})n_{O_2^+}n_{O_2}=f_{O_2},\\
&\alpha_{O_2}n_{O_2^+}n_{O_2}-\gamma_{O_2^+}n_{O_2^+}^2=0,\\
&2\beta_{O_2}n_{O_2^+}n_{O_2}-(\alpha_O+\sigma_{OO^+}v)n_{O_2^+}n_O=0,\\
&\alpha_O n_{O_2^+}n_O-\delta_{O^+}n_{O^+}=0. \qquad \text{(A.1)}
\end{aligned}
$$

In this region, the incident electron fluxes are sufficiently large so that electron impact processes will dominate photolytic processes. We therefore ignore the latter in our polar cap model. We proceed to solve the Eqs. (A.1) and obtain

$$
\begin{aligned}
n_{O_2^+}&=\left[\frac{f_{O_2}\alpha_{O_2}}{\gamma_{O_2^+}(\alpha_{O_2}+\beta_{O_2})}\right]^{1/2},\\
n_{O_2}&=\left[\frac{f_{O_2}\gamma_{O_2^+}}{\alpha_{O_2}(\alpha_{O_2}+\beta_{O_2})}\right]^{1/2},\\
n_O&=\frac{2\beta_{O_2}}{(\alpha_O+\sigma_{OO^+}v)}\left[\frac{f_{O_2}\gamma_{O_2^+}}{\alpha_{O_2}(\alpha_{O_2}+\beta_{O_2})}\right]^{1/2},\\
n_{O^+}&=\frac{\alpha_O 2\beta_{O_2}f_{O_2}}{\delta_{O^+}(\alpha_{O_2}+\beta_{O_2})(\alpha_O+\sigma_{OO^+}v)}. \qquad \text{(A.2)}
\end{aligned}
$$

In the last of these equation, we use an estimate of the escape rate of atomic oxygen ions given by the 18 km s^{-1} velocity inferred by Vasyliūnas and Eviatar (2000) from the published PLS data and an electron depletion length of 200 km.

A.2. The equatorial region

In the equatorial region, $\lambda < 45^\circ$, we have, as discussed in the main text body above, the following set of equations:

$$
\begin{aligned}
H_2O:\ &\frac{j_w}{H_{H_2O}}-((\alpha_{H_2O}+\beta_{H_2O})n_e+\eta^d_{H_2O}\\
&+\eta^i_{H_2O})n_{H_2O}=0,\\
H_2O^+:\ &(\alpha_{H_2O}n_e+\eta^i_{H_2O})n_{H_2O}\\
&-(\gamma_{H_2O^+}n_e+\sigma_{H_2O^+H_2O}v))n_{H_2O^+}=0,\\
H_3O^+:\ &\sigma_{H_2O^+H_2O}vn_{H_2O^+}\\
&-\gamma_{H_3O^+}n_e n_{H_3O^+}=0,\\
OH:\ &((\varepsilon_{OH}(\beta_{H_2O})n_e+\eta^d_{H_2O}))n_{H_2O}+\gamma_{H_2O^+}n_e n_{H_2O^+}\\
&+\gamma_{H_3O^+}n_e n_{H_3O^+}-((\alpha_{OH}+\beta_{OH})n_e+\eta^d_{OH}\\
&+\eta^i_{OH})n_{OH}=0,\\
OH^+:\ &(\alpha_{OH}n_e\eta^i_{OH})n_{OH}\\
&-\gamma_{OH^+}n_e n_{OH^+}=0,\\
O:\ &\varepsilon_O(\beta_{H_2O}n_e+\eta^i_{H_2O})n_{H_2O}\\
&-((\alpha_O+\sigma_{OO^+}v)n_e+\eta^i_O)n_O=0,\\
O^+:\ &(\alpha_O n_e+\eta^i_O)n_O-\psi_s n_O n_{O^+}=0. \qquad \text{(A.3)}
\end{aligned}
$$

In Eq. (A.3) the ε_j factors indicate the branching ratio of the reaction that delivers component j to the system.

This set of equations can be solved with the aid of a few simplifying assumptions which we list in the text.

References

Alexander, C.J., Bolton, S.J., Carlson, R., Ip, W.H., Spencer, J.R., Upward flux of sublimation from the surface of Ganymede. Icarus 1999, submitted for publication.

Bar-Nun, A., Herman, G., Rappaport, M.L., Mekler, Y., 1985. Ejection of H_2O, O_2, H_2 and H from water ice by 0.5–6 kev H^+ and Ne^+ ion bombardment. Surf. Sci. 150, 143–156.

Barth, C.A., Hord, C.W., Stewart, A.I.F., Pryor, W.R., Simmons, K.E., McClintock, W.E., Ajello, J.M., Naviaux, K.L., Aiello, J.J., 1997. Galileo ultraviolet spectrometer observations of atomic hydrogen in the atmosphere of Ganymede. Geophys. Res. Lett. 24, 2147–2150.

Book, D.L., 1977. Revised and enlarged collection of plasma physics formulas and data. Memo. Rep. 3322. Naval Res. Lab., Washington, D.C.

Broadfoot, A., et al., 1981. Overview of the Voyager ultraviolet spectrometry results through Jupiter encounter. J. Geophys. Res. 86, 8259–8285.

Brown, M.E., Boucher, A.H., 1999. Observations of Ganymede's visible aurora. Bull. Amer. Astron. Soc. 31, 1183.

Budzien, S.A., Festou, M.C., Feldman, P.D., 1994. Solar flux variability and the lifetimes of cometary H_2O and OH. Icarus 107, 164–188.

Calvin, W.M., Johnson, R.E., Spencer, J.R., 1996. O_2 on Ganymede: Spectral characteristics and plasma formation mechanisms. Geophys. Res. Lett. 23, 673–676.

Carlson, R.W., Bhattacharyya, J.C., Smith, B.A., Johnson, T.V., Hidavat, B., Smith, S.A., Taylor, G.E., O'Leary, B.T., Brinkman, R.T., 1973. An atmosphere on Ganymede from its occultation of SAO-186800 on 7 June 1972. Science 182, 53–55.

Cosby, P.C., 1993. Electron-impact dissociation of oxygen. J. Chem. Phys. 98, 9560–9569.

Eviatar, A., Lenchek, A.M., Singer, S.F., 1964. Distribution of density in an ion-exosphere of a non-rotating planet. Phys. Fluids 7, 1775–1779.

Eviatar, A., Williams, D.J., Paranicas, C., McEntire, R.W., Mauk, B.H., Kivelson, M.G., 2000. Trapped energetic electrons in the magnetosphere of Ganymede. J. Geophys. Res. 105, 5547–5553.

Feldman, P.D., McGrath, M.A., Strobel, D.F., Moos, H.W., Rutherford, K.D., Wolven, B.C., 2000. HST/SSTIS ultraviolet imaging of polar aurora on Ganymede. Astrophys J. 535, 1085–1090.

Frank, L.A., Paterson, W.R., Ackerson, K.L., Bolton, S.J., 1997. Outflow of hydrogen ions from Ganymede. Geophys. Res. Lett. 24, 2151–2154.

Gurnett, D.A., Kurth, W.S., Roux, A., Bolton, S.J., Kennel, C.F., 1996. Evidence for a magnetosphere at Ganymede from plasma-wave observations by the Galileo spacecraft. Nature 384, 535–537.

Hall, D., Strobel, D.F., Feldman, P.D., McGrath, M.A., Weaver, H.A., 1995. Detection of an oxygen atmosphere on Jupiter's moon Europa. Nature 373, 677–679.

Hall, D.T., Feldman, P.D., McGrath, M.A., Strobel, D.F., 1998. The far-ultraviolet oxygen airglow of Europa and Ganymede. Astrophys. J. Lett. 499, 475–485.

Hendrix, A.R., Barth, C.A., Hord, C.W., 1999. Ganymede's ozone-like absorber: Observations by the Galileo ultraviolet spectrometer. J. Geophys. Res. 104, 14,169–14,177.

Huebner, W.F., Keady, J.J., Lyon, S.P., 1992. Solar photo rates for planetary atmospheres and atmospheric pollutants. Astrophys. Space Sci. 195, 1–294.

Johnson, R.E., 1990. Energetic Charged Particle Interactions with Atmospheres and Surfaces. Physics and Chemistry in Space. Springer, Berlin.

Johnson, R.E., 1996. Sputtering of ices in the outer solar system. Rev. Mod. Phys. 68, 305–312.

Johnson, R.E., 1997. Polar "caps" on Ganymede and Io revisited. Icarus 128, 469–471.

Johnson, R.E., Jesser, W.A., 1997. (O_2/O_3) micro-atmospheres in the surface of Ganymede. Astrophys. J. 480, L79–L82.

Johnson, R.E., Quickenden, T.I., 1997. Photolysis and radiolysis of water ice on outer solar system bodies. J. Geophys. Res. 102, 10,985–10,996.

Kella, D., Johnson, P.J., Pedersen, H.B., Vejby-Christensen, L., Andersen, L.H., 1997. The source of green light emission determined from a heavy-ion storage ring experiment. Science 276, 1530–1533.

Kivelson, M.G., Khurana, K.K., Russell, C.T., Walker, R.J., Warnecke, J., Coroniti, F.V., Polansky, C., Southwood, D.J., Schubert, G., 1996. Discovery of Ganymede's magnetic field by the Galileo spacecraft. Nature 384, 537–541.

Kivelson, M.G., Warnecke, J., Bennett, L., Joy, S., Khurana, K.K., Linker, J.A., Russell, C.T., Walker, R.J., Polanskey, C., 1998. Ganymede's magnetosphere: Magnetometer overview. J. Geophys. Res. 103, 19,963–19,972.

Kliore, A.J., 1998. Satellite atmospheres and magnetospheres. In: Anderson, J. (Ed.), Highlights of Astronomy, Vol. 11B. International Astronomical Union, pp. 1065–1069.

Kumar, S., Hunten, D.M., 1982. The atmospheres of Io and other satellites. In: Morrison, D. (Ed.), Satellites of Jupiter, Space Science. University of Arizona Press, Tucson, pp. 782–806 (Chapter 21).

Lotz, W., 1967. Electron-impact ionization cross sections and ionization rate coefficients for atoms and ions. Astrophys. J. Suppl. XIV, 207–238.

Nagy, A.F., Kim, J., Cravens, T.E., Kliore, A.J., 1998. Hot oxygen corona at Europa. Geophys. Res. Lett. 25, 4153–4155.

Orton, G.S., Spencer, L.D., Martin, T.Z., Tamppari, L.K., 1996. Galileo photopolarimeter-radiometer observations of Jupiter and the Galilean satellites. Science 274, 389–391.

Pappalardo, R.T., et al., 1997. Ganymede tectonics: insights from Galileo imaging. Bull. Amer. Astron. Soc. 29, 989.

Paranicas, C., Paterson, W.R., Cheng, A.F., Mauk, B.H., McEntire, R.W., Frank, L.A., Williams, D.J., 1999. Energetic particle observations near Ganymede. J. Geophys. Res. 104, 17,459–17,469.

Richardson, J.D., Eviatar, A., McGrath, M.A., Vasyliūnas, V.M., 1998. OH in Saturn's magnetosphere, observations and implications. J. Geophys. Res. 103, 20,245–20,256.

Saur, J., Strobel, D.F., Neubauer, F.M., 1998. Interaction of the Jovian magnetosphere with Europa: constraints on the neutral atmosphere. J. Geophys. Res. 103, 19,947–19,962.

Schmidt, H.U., Wegmann, R., Huebner, W.F., Boice, D.C., 1988. Cometary gas and plasma flow with detailed chemistry. Comput. Phys. Commun. 49, 17–59.

Scudder, J.D., Sittler Jr., E.C., Bridge, H.S., 1981. A survey of the plasma electron environment of Jupiter: A view from Voyager. J. Geophys. Res. 86, 8157–8179.

Shulman, M.B., Sharpton, F.A., Chung, S., Lin, C.C., Anderson, L.W., 1985. Emission from oxygen atoms produced by electron-impact dissociative excitation of oxygen molecules. Phys. Rev. A 32, 2100–2115.

Sieveka, E.M., Johnson, R.E., 1982. Thermal and plasma induced molecular redistribution on the icy satellites. Icarus 51, 528–548.

van Dishoeck, E.F., Dalgarno, A., 1984. The dissociation of OH and OD in comets by solar radiation. Icarus 59, 305–313.

Vasyliūnas, V.M., Eviatar, A., 2000. Outflow of ions from Ganymede: a reinterpretation. Geophys. Res. Lett. 27, 1347–1350.

Volwerk, M., Kivelson, M.G., Khurana, K.K., McPherron, R.L., 1999. Probing Ganymede's magnetosphere with field line resonances. J. Geophys. Res. 104, 14,729–14,738.

Walls, F.L., Dunn, G.H., 1974. Measurement of total cross sections for electron recombination with NO^+ and O_2^+ using ion storage techniques. J. Geophys. Res. 79, 1,911–1,915.

Williams, D.J., Mauk, B.H., McEntire, R.W., 1997. Trapped electrons in Ganymede's magnetic field. Geophys. Res. Lett. 24, 2953–2956.

Williams, D.J., Mauk, B.H., McEntire, R.W., 1998. Properties of Ganymede's magnetosphere as revealed by energetic particle observations. J. Geophys. Res. 103, 17,523–17,534.

Yung, Y.L., McElroy, M.B., 1977. Stability of an oxygen atmosphere on Ganymede. Icarus 30, 97–103.